Bioinspiration & Biomimetics



RECEIVED

9 March 2025

16 August 2025

ACCEPTED FOR PUBLICATION
9 September 2025

PUBLISHED 19 September 2025

PAPER

From beetle to bot: bioinspired design of robotic grippers based on stag beetle mandible biomechanics

Mahdi Rajabi^{1,2}, Sepehr H Eraghi¹, Arman Toofani¹, Shayan Ramezanpour¹, Preenjot Singh^{1,4}, Jianing Wu^{5,6}, Chung-Ping Lin⁷ and Hamed Rajabi^{1,3,*}

- $Mechanical \ Intelligence\ (MI)\ Research\ Group, Bioscience\ and\ Bioengineering\ Research\ Centre, London\ South\ Bank\ University, London,\ United\ Kingdom$
- ² Faculty of Mechanical Engineering, University of Guilan, Rasht, Iran
- ³ School of Engineering and Design, College of Technology and Environment, London South Bank University, London, United Kingdom
- ⁴ Integrated Science Education and Research Center (ISERC), Visva Bharati University, West Bengal, India
- School of Advanced Manufacturing, Sun Yat-Sen University, Shenzhen, People's Republic of China
- ⁶ School of Aeronautics and Astronautics, Sun Yat-Sen University, Shenzhen, People's Republic of China
- Department of Life Science, National Taiwan Normal University, No. 88, Sec. 4, Tingzhou Rd, Taipei, Taiwan
- * Author to whom any correspondence should be addressed.

E-mail: rajabijh@lsbu.ac.uk

Keywords: insect weapons, assembly grippers, biomimetics, biomechanics, mechanical intelligence Supplementary material for this article is available online

Abstract

Conventional rigid grippers remain the most-used robotic grippers in industrial assembly tasks. However, they are limited in their ability to handle a diverse range of objects. This study draws inspiration from nature to address these limitations, employing multidisciplinary methods, such as computer-aided design, parametric modeling, finite element analysis, 3D printing, and mechanical testing. Computational analysis of three distinct mandible morphs from the stag beetle Cyclommatus mniszechi revealed that key geometric features—specifically mandible curvature and denticle arrangement—govern a functional trade-off between grasping ability and structural safety. This analysis identified a specific morphology optimized for superior grabbing performance, which served as the template for our design. Leveraging these biological principles, we used parametric modeling to design, and 3D printing to fabricate, a series of novel, mechanically intelligent grippers. Mechanical testing of these prototypes validated our design approach, demonstrating that specific modifications to curvature could significantly enhance the gripper's load-bearing capacity while minimizing object damage. This work establishes a clear pathway from biomechanical analysis to engineered application, offering a robust and cost-efficient blueprint for developing next-generation grippers that operate effectively without complex sensing or actuation systems for tasks in manufacturing, logistics, and healthcare.

1. Introduction

Robotic grippers serve a vital role in various industries, encompassing tasks such as grabbing, holding, displacing, and manipulating objects across industrial, medical, and transportation sectors [1, 2]. Their applications span from assembly tasks and object manipulation to packaging, robotic surgery, and deep-sea exploration [3–5]. Prospects include potential uses in collecting space debris and managing oceanic pollution by retrieving and disposing of debris [6, 7]. Presently, industrial grippers

predominantly fall into two categories: soft and rigid grippers.

Soft grippers offer versatility in handling objects of diverse shapes due to their adaptable nature. However, their design complexity often requires active and continuous actuation and control, typically relying on smart materials. Moreover, they tend to exhibit low energy efficiency, incur high maintenance costs, and lack precision [8, 9]. Conversely, rigid grippers efficiently perform specific tasks but are constrained by drawbacks such as the generation of high output force (also known as manipulation force),

which increases the risk of damaging objects, and a limited ability to grasp objects with varying sizes [8]. Hence, there is an urgent need to devise grippers capable of mitigating the shortcomings associated with existing grippers.

Biological systems offer intriguing solutions, having evolved structures adept at object manipulation. Efforts to replicate such structures in robotic grippers have predominantly centered on mimicking the human hand, albeit with limited success due to challenges in replicating essential properties or resulting in prohibitively expensive solutions [10]. Other approaches have drawn inspiration from soft-bodied organisms; for example, SpiRobs replicate the logarithmic spiral of octopus arms to create flexible, cable-driven manipulators capable of versatile wrapping grasps [11]. Meanwhile, insect mandibles, particularly those of male stag beetles, present a promising alternative [12]. These biological grippers offer simplicity amenable to more effective and efficient modeling compared to the complexities of the human hand. Stag beetle mandibles are specialized tools tailored to the demands of male-male combat, where winning contests relies on secure grasps on opponents of various shapes and sizes.

In this study, employing innovative biomimetic approaches, we explore whether stag beetle mandibles can serve as inspiration for developing mechanical grippers capable of addressing the limitations of existing robotic grippers. We focus on the species Cyclommatus mniszechi due to the distinct morphs exhibited by males within this species (figure 1) and the thorough understanding of their fighting behavior, which extensively involves mandibular usage [13]. Leveraging multidisciplinary methods including computer-aided design, parametric modeling, finite element analysis (FEA), 3D printing, and mechanical testing using a robotic arm, our objectives are twofold: to investigate the relationship between mandible design and mechanical performance and to devise mandible-inspired strategies for enhancing robotic gripper performance. This research represents the pioneering effort in leveraging insect fighting apparatus as templates for improving man-made tools, with implications extending to both robotic gripper design and the elucidation of stag beetle mandible biomechanics [14].

2. Materials and methods

2.1. Mechanical performance of stag beetle mandibles

We utilized digital images of mandibles from adult males of *C. mniszechi* and modeled them using Rhino 7 (Rhinoceros 3D) modeling software. Given that the primary grasping and biting actions of these

mandibles occur within a single plane and their outof-plane curvature is negligible, we opted to model them as two-dimensional (2D) structures (figure S1). This 2D projection approach is a common and effective method in comparative biomechanics for analyzing the performance of planar biological structures, as it efficiently captures the functional trade-offs governed by the in-plane geometry while significantly reducing computational cost and design complexity [15–17].

The 2D mandible models were constructed by projecting their geometry onto a defined 2D coordinate system. We categorized our models into two main and two additional categories. The main categories comprised (1) 'real-size' models, utilized to compare the performance of actual mandibles, and (2) 'same-surface' models, in which we scaled the models to possess the same surface area. We employed the 'same-surface' models for gripper design and to assess mandibles solely based on shape differences, independent of their dimensions. This approach, based on the method outlined by Dumont et al [18], allows for the comparison of models with different shapes while controlling for the effects of size, enabling a clearer understanding of how shape variations influence mechanical performance. Here 'performance' denotes the ability of mandibles to forcefully bite and grasp objects while remaining intact. The additional categories encompassed (1) 'same-length' models, used to isolate the effect of length alone, and (2) 'overlapping' models, where the mandibles could overlap while grasping objects, enabling us to capture the effect of the mandibles' up-down asymmetry on their mechanical performance (figure S2).

For analysis, the developed models were imported into the finite element software package Abaqus (Simulia). Assigning an elastic modulus of 5.1 GPa [19], a Poisson's ratio of 0.3 [19], and a density of 1200 kg m⁻³ [20] to the mandible models, mirroring cuticle material properties. The biting objects were assumed to share identical material properties as the mandibles.

We utilized CPS4R type elements, representing a plane stress element with four integral points, incorporating reduced integration, hourglass control, and distortion control. Hourglass control prevented severe mesh distortions and avoided unrealistic stress concentrations. A mesh convergence analysis was conducted to determine the optimal mesh size balancing simulation accuracy with computational cost. The average number of elements among the models was about 15 000. A representative image of the mesh used is shown in figure S3.

The Abaqus implicit dynamic solver was employed to simulate the mechanical behavior of the models. Surface-to-surface contact between mandibles and objects prevented penetration. A low

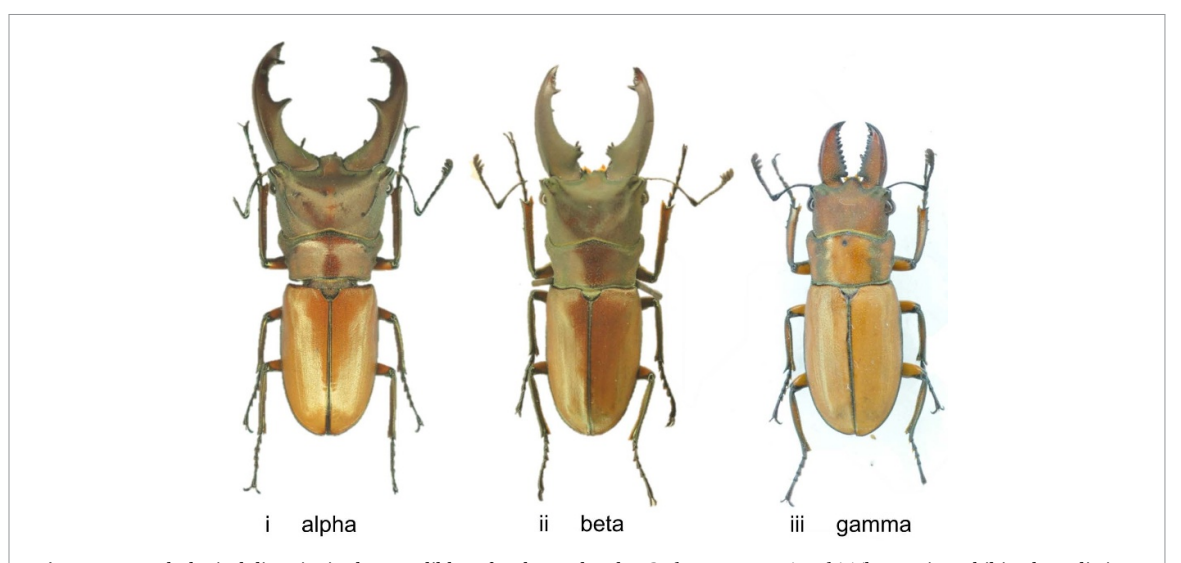


Figure 1. Morphological diversity in the mandibles of male stag beetles *Cyclommatus mniszechi*. The species exhibits three distinct male morphs: (i) alpha, characterized by long, highly curved mandibles with a prominent central denticle; (ii) beta, with shorter, less curved mandibles and several large basal teeth; and (iii) gamma, featuring the shortest and least curved mandibles with numerous small teeth along their length. These morphological differences form the basis for our biomechanical investigation.

coefficient of friction ($\mu=0.05$) was intentionally selected to simulate a 'worst-case' scenario for gripping. This approach minimizes the contribution of friction and forces the grippers to rely primarily on their geometric features (i.e. mechanical interlocking from denticles and curvature) to secure an object, allowing for a more robust evaluation of the shape's performance.

To computationally estimate the biting and grabbing forces of the mandibles, it was essential to employ loading and boundary conditions that accurately replicated the dynamics of fights (figure S1). Simulations were conducted in a two-step process. Initially, a normal unit force was applied to the mandible base, where closing muscles are attached. Mandibles were permitted to rotate around their hinge under the effect of the applied force until the mandibles made contact with a biting object. (video S1). Circular objects, at five distinct diameters, representing cross sections of different body parts of rivals were utilized as biting objects. The smallest and largest objects corresponded to the cross section of rivals' tibia and thorax, respectively. To optimize computational efficiency, we imposed symmetric boundary conditions and modeled the circular biting objects as semi-circles. Although objects could move upon contact, their movement was constrained by the mandibles. Complete restriction of an object's movement by a mandible indicated a successful grasp. In this phase, the reaction forces at the contact point were measured relative to a coordinate system aligned with the insect's body, where the imaginary body axis was defined as the longitudinal axis running through the center of the beetle's thorax, parallel to the pronotum's midline. The biting force (F_b) was defined

as the force component perpendicular to the insect's imaginary body axis. In the subsequent step, once objects were fully stabilized, an increasing force was applied to the object to pull it away from the mandibles. The grabbing force (F_g) was defined as the component of this pulling force parallel to the insect's imaginary body axis that the mandibles could resist at the onset of opening.

Using the simulation results, we evaluated four mechanical metrics: the quantity of objects seized by each mandible (n), biting force (F_b) , grabbing force (F_g) , and maximum principal stress. The maximum principal stress represents the highest normal stress experienced by the mandibles under loading. While our simulations operate within the linear elastic domain, we used this stress value to calculate a comparative factor of safety (FS). The FS was defined as the ratio of the ultimate tensile strength of insect cuticle (here assumed to be 150 MPa, a value within the typical range reported for cuticle, i.e. 100-200 MPa [20]) to the maximum principal stress developed within the models. This provides a standardized metric for comparing structural integrity.

Given the diverse range of object sizes, multiple locations where mandibles could grasp objects (i.e. base, middle, and tip), and the morphological variations and design complexities inherent in the studied mandible morphs, we evaluated the overall performance of the mandibles by assigning a score to each of the four mechanical metrics (i.e. n, F_b , F_g , FS). Initially, the results for each metric were normalized using the min-max normalization method, a data preprocessing technique that rescales the range of the dataset to a specified range, here [0, 1]. Subsequently, the overall score for each mandible was computed as

the sum of the scores for grasping objects at the base, middle, and tip of the mandible. This method was chosen to provide a comprehensive assessment of the mandible's performance across different object sizes and grasping locations. For example, to determine the biting force (F_b) of the alpha model, we calculated the overall biting force (F_b) by summing the biting scores at the base, middle, and tip for all distinct object sizes separately. This same process was applied to assess the overall n, F_g , and FS (tables S1–S6).

2.2. Parametric modeling

We selected the alpha morph mandibles as our reference model due to their demonstrated superior performance. Utilizing the state-of-the-art parametric modeling plugin Grasshopper within the Rhino 7 software, we created a parametric model of the alpha mandible. This parametric model facilitated the development of a range of mandibleinspired designs by manipulating various design parameters. Specifically, we varied parameters such as inner curvature, outer curvature, denticle length, and denticle location, with the specific ranges for these variations detailed in the supplementary materials (table S12). These models were instrumental in investigating the impact of each parameter on mandible performance metrics, including grabbing force, biting force, FS, and the number of objects gripped.

2.3. Fabrication and mechanical testing

We manufactured the most promising mandibleinspired designs identified through parametric modeling and subjected them to testing within a custom setup. Initially, we prepared the .stl files of the models for 3D printing using the advanced slicing software IdeaMaker by Raise3D. Employing adaptive tools that offered precise control over printing parameters, we optimized aspects such as layer height, infill pattern, infill density, support structure, and surface quality enhancement. To transition from 2D to 3D models, we gave the selected designs depth, converting them into fully three-dimensional representations suitable for physical testing. 3D printing was chosen as a costeffective and time-efficient prototyping method, with polylactic acid (PLA) filament ($E \approx 3.5$ GPa) selected for its high strength-to-weight ratio. It is important to note that the goal of these experiments was to validate the relative performance ranking of the computationally-derived designs, not to replicate the absolute force values from the simulations which used cuticle material properties.

Subsequently, the models were fabricated using a fused deposition modeling 3D printer (Raise3D E2). These manufactured parts were then integrated into a customized rack and pinion mechanism designed to convert linear motion generated by a robotic arm (Dobot Magician) into rotary motion (figure S4). The robotic arm's function was to operate the mandible-inspired grippers, enabling them to open, close, and

interact with a set of 3D printed cylindrical objects (video S2). The absolute dimensions and mass for each of the 3D-printed gripper designs are provided in the supplementary materials (table S13).

Our experimental focus centered on assessing the load-bearing capacity of the mandible-inspired grippers, particularly in terms of their ability to lift objects of varying weights. All objects were made using PLA, the same material that we used for 3D printing of the grippers. These objects had the same size and shape, but different weights were applied by hanging them from the objects (figure 4; video S2). This directly corresponded to evaluating the gripping performance of the grippers. The results obtained were utilized to compare the performance of different mandible-inspired designs within practical applications.

3. Results

3.1. Morphology of the mandibles

We conducted an examination of the geometric parameters of the mandibles from three morphs, namely alpha, beta, and gamma, of the stag beetle *C. mnisze-chi* (figure 1). These mandibles exhibit variations across four key geometric parameters: (1) aspect ratio, (2) inner curvature, (3) outer curvature, and (4) denticles. The denticles on each mandible were characterized based on three parameters: their number, length, and spacing both between each other and from the base.

In the gamma mandible, all denticles are small and arranged along the entire length, except for a small area at the base (figure 1). Conversely, in the alpha and beta mandibles, most small denticles are concentrated in the region between two large distal denticles, with the beta mandible featuring a few large teeth in the basal part, unlike the alpha mandible, which lacks teeth in this region and instead exhibits a prominent denticle in the middle region.

Geometric analysis revealed that gamma and alpha mandibles possess the highest (n=16) and lowest (n=8) number of denticles, respectively (figure 1). The method outlined in [21] was employed to measure both the inner and outer curvatures of the mandibles. Alpha mandible exhibited the highest inner and outer curvatures, followed by beta and gamma mandibles, respectively (figure 1). Additionally, the alpha mandible displayed the largest aspect ratio (length/width) (AR = 2.68), while the gamma mandible featured the smallest aspect ratio (AR = 2.4).

3.2. Mechanical behavior of mandibles

Using FEA, we conducted a comprehensive comparative study and evaluated the mandibles based on their overall performance in handling a variety of objects (see materials and methods). The results from the numerical study are detailed in tables S1–S6, and key observations are presented here. None of the

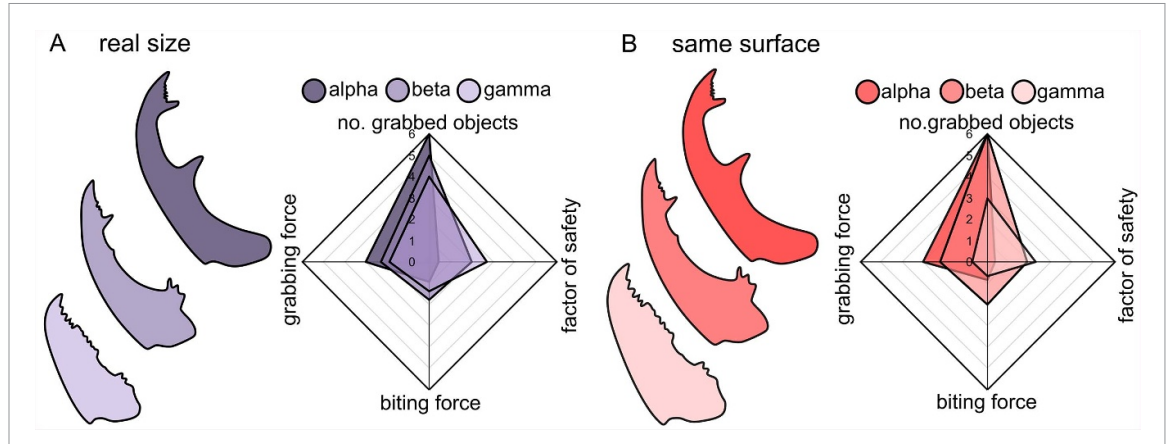


Figure 2. Comparative biomechanical performance of the three mandible morphs. The radar plots show the overall performance scores for four metrics: number of grabbed objects, grabbing force, biting force, and factor of safety. (A) Performance of the mandibles at their actual biological size. The alpha mandible excels in grabbing force and the number of objects grasped, while the gamma mandible has the highest factor of safety. (B) Performance of mandibles scaled to the same surface area to isolate the effect of shape. The results confirm that the alpha mandible's geometry is inherently superior for grasping, validating its selection as a design template.

mandibles were able to grasp the largest object, corresponding to the thorax of the stag beetles. This object represents the circumference of the thorax at its largest part, which is not typically grabbed by stag beetles during fights. Instead, the insects usually grab the hinges between the body segments. Therefore, the inability to grasp this object reflects the natural behavior of stag beetles.

3.2.1. Mechanical performance of the mandibles in their real size

The findings from the FEA of the mandibles in their real size for the alpha, beta, and gamma morphs are presented in figure 2(A) and table S1. Regarding the number of objects grasped (n), the alpha mandible outperformed the others, grabbing six objects compared to five objects grabbed by the beta mandible and four objects for the gamma mandible (figure 2(A), table S1). In terms of biting force (F_b) , the beta mandible demonstrated the highest performance, nearly double that of the alpha mandible. The alpha mandible, however, achieved the highest grabbing force (F_g) , surpassing the gamma mandible by 1.6 times. The gamma mandible exhibited the highest FS, being 6.2 times that of the alpha mandible and 1.3 times that of the beta mandible (figure 2(A), table S1).

In summary, the alpha mandible demonstrated superior capabilities in grabbing objects, excelling in both the quantity of objects grabbed and grabbing force, although it exhibited the lowest biting force and FS. The gamma mandible, on the other hand, had the highest FS but the lowest grabbing force and ability to grab objects.

3.2.2. Mechanical performance of the mandibles with the same surface area

To isolate the effect of shape from size, we also analyzed models scaled to the same surface area and

length (figure 2(B), tables S2 and S3). These analyses confirmed the superior grabbing performance of the alpha mandible's shape. The beta mandible consistently generated the highest biting force, while the gamma mandible had the highest FS. We also explored the effect of up–down asymmetry using overlapping models (figure S2; tables S4–S6), which showed improved grabbing for all morphs but maintained the same relative performance ranking.

Collectively, these simulations demonstrate a clear functional trade-off: the alpha mandible's morphology is optimized for grasping a wider range of objects and generating high grabbing force, albeit at the cost of lower biting force and FS. Based on these findings, which highlight its superior grasping capabilities, we selected the alpha mandible as the template for our bioinspired gripper design.

3.3. Mandible-inspired design of a robotic gripper

Our biomechanical analysis revealed that the alpha mandible's geometry is specialized for superior grabbing. To translate this biological insight into an engineered system, we aimed to design a gripper that retains the alpha mandible's high grabbing force (F_g) and ability to handle multiple objects (n), while simultaneously improving its FS and minimizing the risk of object damage by reducing its biting force (F_b).

Therefore, we established our design priorities in the following order: (1) achieving a higher number of grabbed objects (n), (2) attaining a greater grabbing force (F_g) , (3) minimizing biting force (F_b) (expressed as the inverse of biting force, $1/F_b$, where a higher $1/F_b$ indicates reduced potential damage caused by the gripper to the seized objects), and (4) ensuring a higher FS.

Guided by the specified criteria, we designated the alpha mandible as the reference model (referred to as model c, figure 3). Subsequently, we developed a

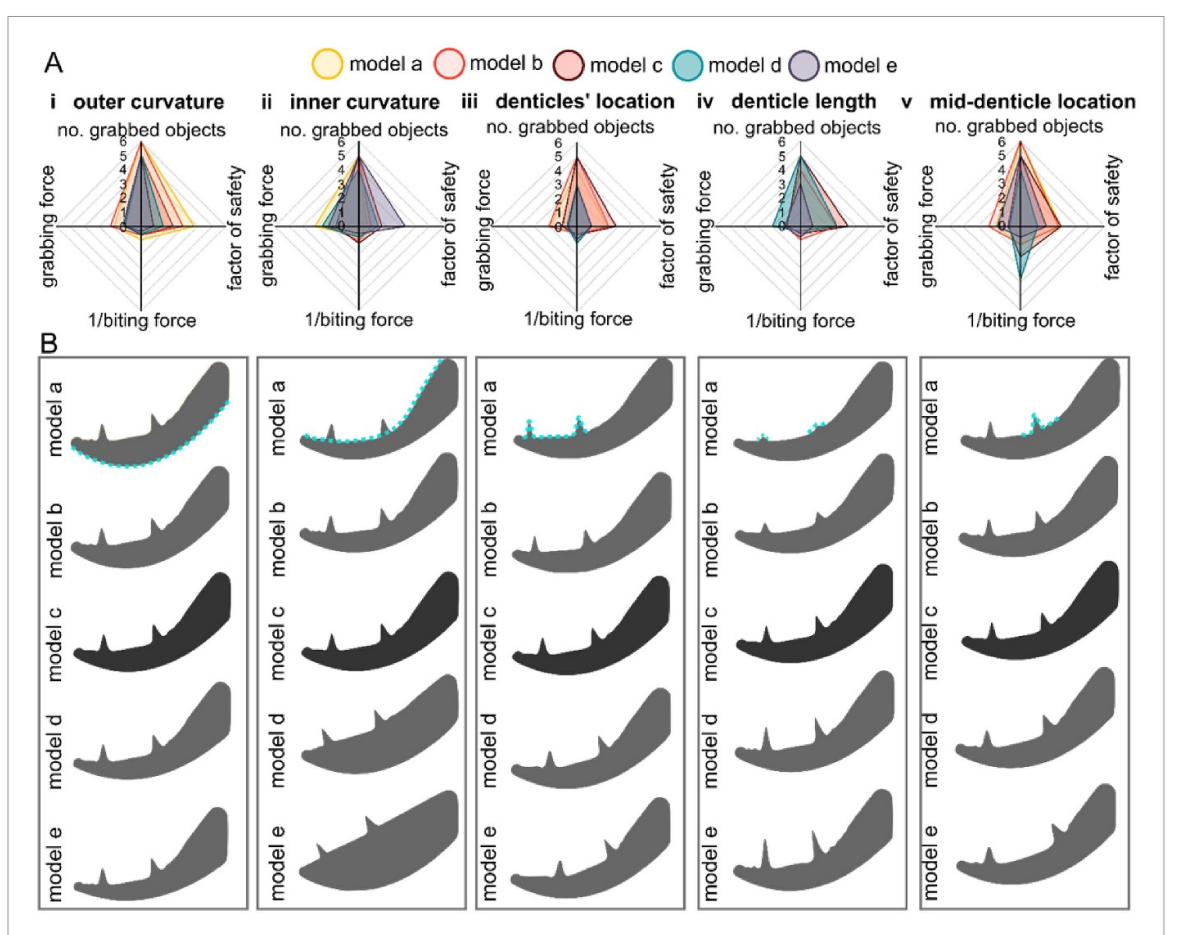


Figure 3. Parametric analysis of gripper geometry based on the alpha mandible. (A) Radar plots showing the performance of modified gripper designs. The four axes represent our design priorities: number of grabbed objects (n), grabbing force (F_g) , inverse of biting force $(1/F_b)$, and factor of safety (FS). (B) The geometric variations tested. The central model in each column (model c) is the original alpha mandible. Designs were varied by systematically altering five key parameters: (i) outer curvature, (ii) inner curvature, (iii) location of all denticles, (iv) length of all denticles, and (v) location of the mid-denticle. This analysis reveals how specific geometric changes impact performance, guiding the selection of optimized gripper designs.

parametric model of the alpha mandible, allowing us to modify design parameters, namely outer curvature, inner curvature, denticles' location, denticles' length, and mid-denticle's location—within a reasonable range (figure 3(B)). For each adjusted design parameter, we generated five models by both increasing and decreasing the corresponding parameter in two iterations relative to model c. In total, 21 models were created for the comparative FEA (figure 3(B), tables S7–11).

Number of grabbed objects (n)

The results of our comparative analysis revealed that the location and length of the denticles had the most significant influence on the gripper's ability to grab objects (n) (figures 3(A iii), (iv))—while the models with the outer curvature variations could grasp between 5 to 6 objects, changing the other two design parameters (denticle length and location) resulted in a wider range of grabbed objects, from 0 to 5. In contrast, the inner curvature exhibited the least impact on the number of the grabbed

objects (n) (figure 3(Aii)). Both increasing (by 1.8 times) and decreasing (by 4.4 times) the length of the denticles resulted in a reduction in n, indicating that the reference model (model c) could grab a greater number of objects. In model a, where the denticles are nearly absent, the gripper was incapable of grabbing any objects. Similarly, relocating the two denticles towards both the tip and base of the gripper decreased n.

1/Biting force $(1/F_b)$

Our findings demonstrated that nearly all design parameters had an influence on the inverse of biting force $(1/F_b)$ but to varying degrees (figure 3(A)). Shifting the mid-denticle towards the base of the gripper increased $1/F_b$ by 2.74 times. Similarly, a substantial increase in outer curvature elevated $1/F_b$ by 2.70 times. Regarding inner curvature, both its increase and decrease relative to the reference model (model c) enhanced $1/F_b$ by 1.70 and 2.15 times, respectively. Furthermore, alterations in the length of denticles exhibited a nonlinear

effect on $1/F_b$, with a reduction in length leading to zero biting force when the denticles disappeared, signifying a substantial decrease in the biting force.

Grabbing force (F_g)

The location of the denticles, inner curvature, and outer curvature had the most significant impact on the gripping force $(F_{\rm g})$ of the gripper. Specifically, relocating both denticles towards the tip of the gripper resulted in a 3.6-fold improvement in $F_{\rm g}$. Adjustments in the inner curvature, involving both increases and decreases, enhanced $F_{\rm g}$ by 1.9 and 1.3 times, respectively. Similarly, modifications in the outer curvature, encompassing both increases and decreases, led to improvements in $F_{\rm g}$ by 1.7 and 0.9 times, respectively.

FS

Regarding the FS, the FEA results indicated that inner curvature, outer curvature, and length of denticles were highly impactful design parameters. Notably, increasing the inner curvature and outer curvature substantially increased the FS by 6.2 and 4.2 times, respectively. Conversely, increasing the length of denticles decreased the FS by 3.9 times. Additionally, relocating both denticles towards the base and tip of the gripper resulted in a reduction in FS, indicating that the reference model (model c) exhibited a higher FS.

Bioinspired design

Based on the findings from our parametric study, we selected eight distinct gripper designs (referred to as grippers 1–8) for fabrication and experimental validation. The selection process was guided by our design priorities and aimed to explore different performance trade-offs identified in the simulations. The rationale for each design is as follows:

- Gripper 1 (baseline): the original alpha mandible geometry was selected as the baseline to represent the best-performing natural design for grasping.
- Gripper 2 (maximum versatility): this design combines the features of the models that demonstrated the ability to grasp the highest number of objects (*n* = 6) in our simulations. Specifically, it is based on model 'a' from the outer curvature variations (figure 3(Ai)) and model 'a' from the mid-denticle location variations (figure 3(Av)).
- Gripper 3 (combined optimum): this design is a composite that integrates the geometric features that individually yielded the best performance across all four metrics: the outer curvature from

the model with the highest 'n', the inner curvature from the model with the highest FS, and so on. This represents a theoretical 'best-of-all-worlds' approach.

In addition to the above, we selected the most optimal models from each category in the comparative FEA study in terms of their overall performance (figure 3):

- Gripper 4 (high grabbing force & low biting force): this design is based on model 'a' from the inner curvature variations (figure 3(Aii)), chosen for its excellent combination of high grabbing force (F_g), number of grabbed objects (n = 5), and low bite force (F_b).
- Gripper 5 (delicate handling): this design is based on model 'd' from the denticle length variations (figure 3(Aiv)). It was selected because it produced one of the lowest biting force (highest 1/F_b), making it the most suitable candidate for grasping delicate objects without causing damage.
- Gripper 6 (balanced performance): this design is based on model 'b' from the denticle location variations (figure 3(Aiii)). It was chosen for its strong, balanced performance across all four metrics, representing a versatile, general-purpose design.
- Gripper 7 (alternate balanced performance): this design is based on model 'b' from the middenticle location variations (figure 3(Av)), which also exhibited a very low biting force (high $1/F_b$), a high number of grabbed objects (n=6), high grabbing force (F_g), and its high FS, providing an alternative strategy for delicate manipulation.
- Gripper 8 (Robust & Versatile): this design is based on model 'a' from the outer curvature variations (figure 3(Ai)), selected for its high FS and ability to grasp a high number of objects (*n*), making it a robust and versatile option.

To assess their grabbing capabilities, we first 3D-printed the designed grippers and then attached them to a robotic arm. Next, we created a circular object, to which various weights were attached, and utilized them to evaluate the load-bearing capacity of the grippers (figure 4, video S2). Grippers 4 and 8 exhibited the highest load-bearing capacity, as they were capable of grabbing and lifting objects weighing up to 120 g, indicating that increasing both inner and outer curvatures substantially enhances the load-bearing capacity of the grippers. Furthermore, Grippers 3 and 6 demonstrated the lowest load-bearing capacity, supporting a weight of 50 g (figure 4).

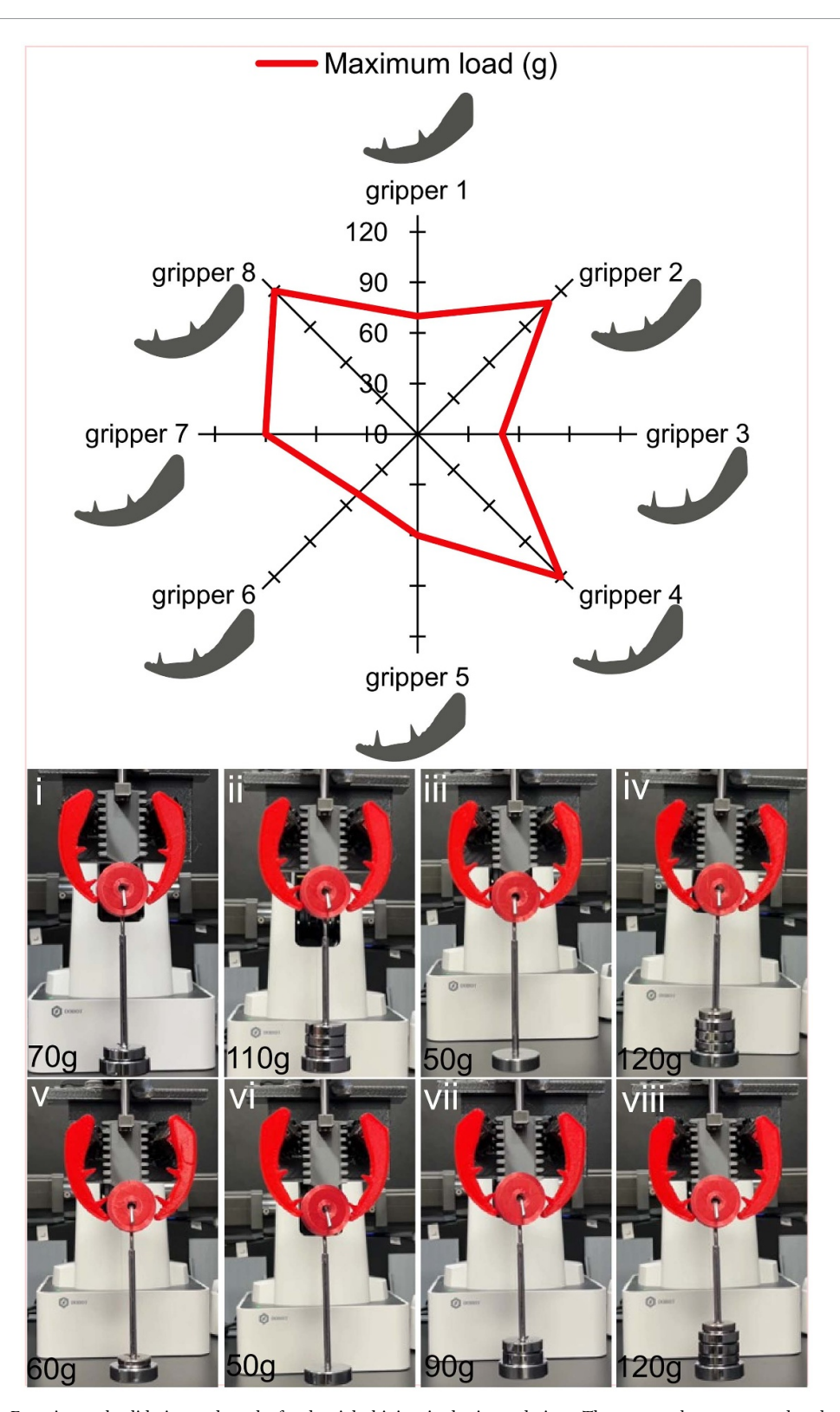


Figure 4. Experimental validation and results for the eight bioinspired gripper designs. The top panel presents a radar plot summarizing the maximum load-bearing capacity (in grams) for each design. The bottom panel (i)–(viii) shows the experimental setup for each corresponding gripper, capturing the moment it successfully lifts its maximum supported weight. The results demonstrate a clear performance difference between the designs, with Grippers 4 (iv) and 8 (viii) exhibiting the highest capacity (120 g), confirming that the geometric modifications identified in our simulations successfully enhanced performance.

4. Discussion

Male stag beetles use their mandibles as fighting tools to access food, territory and mates [22–25]. Their

mandibles represent a wide range of morphs and sizes [12, 22, 26, 27]. Focusing on distinct mandibles of three morphs of the stag beetle *C. mniszechi*, here we asked how and why they differ in performance and

how they can inform the development of grippers with enhanced gripping ability.

Among the morphs examined in our study alpha, beta, and gamma-each displayed unique characteristics influencing their mechanical performance. Alpha mandible emerged as the most effective in terms of grabbing objects, despite exhibiting lower biting force and FS compared to beta and gamma mandibles. This superiority can be attributed to specific design parameters inherent in the alpha morph. Specifically, while alpha mandible exhibited a lower number of teeth compared to the beta and gamma mandibles, it displayed distinct teeth distribution patterns. Teeth in alpha mandible are concentrated in regions that may play a crucial role in grasping, particularly between two large distal denticles. This arrangement likely enhances the mandible's ability to firmly grasp and manipulate objects, a feature that could contribute to the higher fighting success observed in alpha males [13]. While this hypothesis aligns with observations of mandible morphology in stag beetles, further studies are needed to empirically test how the concentration and configuration of teeth and denticles contribute to grasping efficiency and overall performance in handling objects.

Additionally, the alpha mandible demonstrated greater curvature, both inner and outer, as well as the largest aspect ratio (length/width ratio) among the morphs. This combination of features may enhance its grasping capabilities by providing greater reach and contact area. A larger aspect ratio (longer mandibles) facilitates the mandible's ability to interact with larger objects and potentially offers better leverage for manipulating them. The trade-off, however, is that the force exerted at the tip of the mandible is reduced due to the longer lever arm, resulting in a lower mechanical advantage. This means that while the mandible can handle larger objects, the efficiency of force transmission may decrease, necessitating greater muscle force for manipulation. It is important to mention that our analyses did not show a correlation between the length of the mandibles and the number of the objects they could grab (figure S5).

Our investigation into the morphological and mechanical properties of the mandibles across the three stag beetle morphs reveals interesting connections to the previously documented fighting behaviors. The study by Chen et al [13] demonstrated that alpha morphs exhibited a higher tendency to escalate fights and displayed more aggressive behaviors compared to beta and gamma morphs. Our findings on mandible morphology and mechanics align with this observation. The alpha mandible exhibited superior ability to grasp objects (possibly body parts of rivals) but possessed a lower biting force. This suggests a trade-off between maneuverability (the ability to control and adjust grip during object manipulation) and raw power. In contrast, the beta and gamma mandibles displayed lower grasping abilities but possessed significantly higher safety factors. This could indicate a more defensive fighting style, prioritizing structural integrity over offensive maneuvers. While our findings suggest that the mandible morphology and biomechanics of the morphs may influence their specialized fighting styles, this connection remains speculative. Further studies investigating the correlation between mandible morphology, mechanics, and real-world fighting behaviors would be valuable in solidifying this connection.

In our investigation, we adopted a bioinspired design approach, drawing inspiration from the remarkable grasping capabilities of stag beetle mandibles. We explored the link between key morphological features and mechanical performance across three distinct mandible morphs. Through computational analysis, we identified inner and outer curvatures, along with denticle position and length, as critical parameters influencing grasping, biting force, and structural integrity. The alpha mandible, characterized by high curvatures and prominent denticles, excelled in object grasping but exhibited a lower biting force and FS. In contrast, the gamma mandible, with lower curvatures and smaller denticles, prioritized safety but displayed weaker grasping capabilities. These insights provided a valuable foundation for the development of bioinspired grippers. A key challenge in designing rigid grippers with features like denticles is the potential for damaging the grasped object. To address this directly, our design process explicitly prioritized minimizing the biting force (F_b) while maximizing the grabbing force (F_g) , ensuring a secure grip without exerting excessive, damaging pressure. This principle guided our parametric study and the selection of the final designs.

Utilizing this knowledge, we designed and fabricated a series of bioinspired grippers. Using the alpha mandible as a reference, we created a parametric model to explore the impact of manipulating key design parameters. All manipulated design parameters influenced the performance of the reference model in our parametric study, but in some cases, the changes observed were more notable. For example, the number of grabbed objects was most influenced by the length of the denticles, as reducing the denticle length rendered the gripper unable to grab objects. Similarly, grabbing force was most influenced by the location of the denticles, as mandibles with denticles at the more distal parts could generate higher grabbing forces. Moreover, the defined performance of 1/(biting force) was influenced the most by the location of the middle denticle, as shifting the mid-denticle towards the base of the mandible up to a certain point increased the 1/(biting force). Almost all design parameters influenced the FS of the mandibleinspired gripper; however, the most notable influence was caused by the inner curvature. Reducing the inner curvature step by step led to the increase of the FS. Building upon these results, we 3D-printed

and tested eight gripper designs. The most successful models, exhibiting superior load-bearing capacity, corresponded to those with increased inner and outer curvatures, aligning with computational predictions. This successful experimental validation, despite the difference in material properties between the PLA prototypes and the simulated cuticle, confirms that our FEA-based approach was effective at identifying functionally superior geometries. This successful application of biomimetic principles demonstrates the potential for developing novel grippers with enhanced grasping capabilities and improved safety.

It is important to note that our study involves certain simplifications. Our use of 2D models, while justified for this planar system, does not capture potential out-of-plane stresses. Furthermore, our FEA was limited to the linear elastic domain and did not model plastic deformation or fracture. Consequently, the calculated FS serves as a comparative metric for structural integrity rather than a prediction of absolute failure points. Similarly, the loading scenarios employed in this study were simplified for other design-related purposes. Stag beetles and other insects use their mandibles in a far more complex manner, involving combined loading scenarios such as pulling, pushing, bending, and twisting. These varied loading conditions reflect the dynamic nature of mandible usage, which includes gripping, lifting, and manipulating various shaped body parts of opponents. Future studies should aim to incorporate these complexities to provide a more realistic representation of mandible biomechanics. This would involve testing a wider range of object shapes and other biologically relevant loading scenarios. By exploring these complexities, we can further refine the design of bioinspired grippers, enabling their application in a broader range of practical, real-world scenarios, such as handling irregularly shaped objects or performing tasks that require multidirectional forces.

To further explore the versatility of our designs, we conducted additional simulations on grasping performance with non-circular objects (triangles and squares), using a subset of our most distinct gripper models (figure S6). The results showed that the relative performance of the grippers remained consistent across these different geometries, reinforcing the robustness of our design principles. These findings align with the load-bearing capacities determined experimentally with cylindrical objects, suggesting the performance benefits are not limited to a single object shape. While a comprehensive experimental validation with a wider range of materials (e.g. soft and rigid) and complex geometries is an important avenue for future work, this analysis provides strong evidence for the general applicability of our bioinspired approach.

Stag beetle mandibles and our artificial grippers are great examples of the concept of mechanical

intelligence (MI), which integrates intelligence directly into the design itself. MI refers to the ability of a mechanical system to perform tasks without requiring complex control systems [28]. By embedding MI into the design of the grippers, we achieved gripping performance with minimal reliance on actuators or control mechanisms. This reduces the need for continuous control and minimizes the risk of damage to objects, compared to traditional rigid grippers, which often require precise force control and rely on actuators for every movement. As a result, MIbased grippers are cost-effective, lightweight, and versatile, capable of handling a wider variety of objects [6, 29–33]. This approach has the potential to offer a more efficient and adaptive solution for handling a diverse range of materials and shapes in real-world applications—an area we plan to explore in future studies. Furthermore, developing a complete analytical model of the gripper's mechanics, informed by the key parameters identified in our study, would be a valuable next step for optimizing performance and is a promising avenue for future research.

In conclusion, this study presents a significant step forward in bioinspired gripper design by translating the remarkable grasping capabilities of stag beetle mandibles into the engineering world. Our findings on the critical role of curvatures and denticle parameters provide valuable insights for optimizing grasping performance, biting force, and safety in grippers. This knowledge can be directly applied to the development of next-generation grippers for industrial applications, fostering the creation of versatile tools that overcome the limitations of both soft and rigid grippers. Furthermore, this research represents a pioneering effort in drawing inspiration from insect fighting structures to develop man-made tools [14]. By bridging the gap between biological and engineered grasping systems, this work opens avenues for further exploration in biomimetic design, not only for grippers but potentially for other manipulation tasks as well.

Data availability statement

All data that support the findings of this study are included within the article (and any supplementary files).

Funding

This study was financially supported by the Royal Society Research Grant (Grant No. RGS\R2\222025), the Royal Society International Exchanges Cost Share Grant (Grant No. IEC\R3\213049) to HR, and the National Science and Technology Council (NSTC) Research Grant (Grant No. NSTC 113-2311-B-003-003) to C-PL.

Author contribution

Conceptualization: JW, C-PL, HR; Formal Analysis: MR, SHE, AT, SR, PS; Funding Acquisition: HR, C-PL; Methodology: SHE, AT, SR, C-PL, HR; Resources: HR, C-PL; Supervision: HR; Visualization: AT; Writing—Original Draft: MR, SHE, HR; Writing—Review and Editing: AT, SR, PS, JW, C-PL.

Conflict of interest

The authors declare no competing interests.

ORCID iDs

Sepehr H Eraghi © 0000-0003-4919-0370 Arman Toofani © 0000-0003-1219-7480 Jianing Wu © 0000-0003-0902-4466 Chung-Ping Lin © 0000-0003-2331-8591 Hamed Rajabi © 0000-0002-1792-3325

References

- [1] Beyeler F, Bell D J, Nelson B J, Sun Y, Neild A, Oberti S and Dual J 2006 Design of a micro-gripper and an ultrasonic manipulator for handling micron sized objects 2006 IEEE/RSJ Int. Conf. on Intelligent Robots and Systems (IEEE) pp 772–7
- [2] Belfiore N P, Verotti M, Crescenzi R and Balucani M 2013 Design, optimization and construction of MEMS-based micro grippers for cell manipulation 2013 Int. Conf. on System Science and Engineering (ICSSE) (IEEE) pp 105–10
- [3] Pettersson A, Davis S, Gray J O, Dodd T J and Ohlsson T 2010 Design of a magnetorheological robot gripper for handling of delicate food products with varying shapes J. Food Eng. 98 332–8
- [4] Stephan M, Rognini G, Sengul A, Beira R, Santos-Carreras L and Bleuler H 2010 Modeling and design of a gripper for a robotic surgical system integrating force sensing capabilities in 4 DOF ICCAS 2010 (IEEE) pp 361–5
- [5] Mazzeo A, Aguzzi J, Calisti M, Canese S, Vecchi F, Stefanni S and Controzzi M 2022 Marine robotics for deep-sea specimen collection: a systematic review of underwater grippers Sensors 22 648
- [6] Zhang J, Hu Y, Li Y, Ma K, Wei Y, Yang J, Wu Z, Rajabi H, Peng H and Wu J 2022 Versatile like a seahorse tail: a bio-inspired programmable continuum robot for conformal grasping Adv. Intell. Syst. 4 2200263
- [7] Ruotolo W, Brouwer D and Cutkosky M R 2021 From grasping to manipulation with gecko-inspired adhesives on a multifinger gripper Sci. Robot. 6 eabi9773
- [8] Samadikhoshkho Z, Zareinia K and Janabi-Sharifi F 2019 A brief review on robotic grippers classifications. In 2019 IEEE Canadian Conf. of Electrical and Computer Engineering (CCECE) (IEEE) pp 1–4
- [9] Shintake J, Cacucciolo V, Floreano D and Shea H 2018 Soft robotic grippers Adv. Mater. 30 1707035
- [10] Vittor T, Staab H, Breisch S, Soetebier S, Stahl T, Hackbarth A and Kock S 2011 A flexible robotic gripper for automation of assembly tasks: a technology study on a gripper for operation in shared human environments 2011 IEEE Int. Symp. on Assembly and Manufacturing (ISAM) (IEEE) pp 1–6
- [11] Wang Z, Freris N M and Wei X 2025 SpiRobs: logarithmic spiral-shaped robots for versatile grasping across scales *Device* 3 100646

- [12] Saif N B, Guilani R J A, Ramezanpour S, Toofani A, Eraghi S H, Goss G, Lin C-P, Gorb S and Rajabi H 2025 Engineering the battle: design-specific analysis of stag beetle mandibles for combat efficiency *PNAS Nexus* 4 pgaf205
- [13] Chen Z-Y, Hsu Y and Lin C-P 2020 Allometry and fighting behaviour of a dimorphic stag beetle Cyclommatus mniszechi (Coleoptera: Lucanidae) *Insects* 11 81
- [14] Wipfler B, Hoepfner O, Viebahn F, Weihmann T, Rieg F and Engelmann C 2024 Understanding the ant's unique biting system can improve surgical needle holders *Proc. Natl Acad.* Sci. 121 e2201598121
- [15] Snively E R I C, Anderson P S and Ryan M J 2010 Functional and ontogenetic implications of bite stress in arthrodire placoderms *Kirtlandia* 57 53–60
- [16] Rayfield E J 2011 Structural performance of tetanuran theropod skulls, with emphasis on the megalosauridae, spinosauridae and carcharodontosauridae Special Papers in Palaeontology 86 241–53
- [17] Qian Z, Yang M, Zhou L, Liu J, Akhtar R, Liu C, Liu Y, Ren L and Ren L 2018 Structure, mechanical properties and surface morphology of the snapping shrimp claw *J. Mater. Sci.* 53 10666–78
- [18] Dumont E R, Grosse I R and Slater G J 2009 Requirements for comparing the performance of finite element models of biological structures *J. Theor. Biol.* 256 96–103
- [19] Rajabi H, Jafarpour M, Darvizeh A, Dirks J-H and Gorb S N 2017 Stiffness distribution in insect cuticle: a continuous or a discontinuous profile? J. R. Soc. Interface 14 20170310
- [20] Vincent J F V and Wegst U G K 2004 Design and mechanical properties of insect cuticle Arthropod Struct. Dev. 33 187–99
- [21] Birn-Jeffery A V, Miller C E, Naish D, Rayfield E J, Hone D W E and Dodson P 2012 Pedal claw curvature in birds, lizards and Mesozoic dinosaurs—complicated categories and compensating for mass-specific and phylogenetic control *PLoS One* 7 e50555
- [22] Emlen D J 2008 The evolution of animal weapons *Annu. Rev. Ecol. Evol. Syst.* **39** 387–413
- [23] Inoue A and Hasegawa E 2013 Effect of morph types, body size and prior residence on food-site holding by males of the male-dimorphic stag beetle *Prosopocoilus inclinatus* (Coleoptera: Lucanidae) *J. Ethol.* 31 55–60
- [24] Goyens J, Dirckx J and Aerts P 2015 Stag beetle battle behavior and its associated anatomical adaptations J. Insect Behav. 28 227–44
- [25] Songvorawit N, Butcher B A and Chaisuekul C 2018 Resource holding potential and the outcome of aggressive interactions between paired male Aegus chelifer chelifer (Coleoptera: lucanidae) stag beetles J. Insect Behav. 31 347–60
- [26] Shapiro L H 2000 Reproductive costs to heterospecific mating between two hybridizing katydids (Orthoptera: Tettigoniidae) Ann. Entomol. Soc. Am. 93 440–6
- [27] Shiokawa T and Iwahashi O 2000 Mandible dimorphism in males of a stag beetle, prosopocoilus dissimilis okinawanus (Coleoptera: Lucanidae) Appl. Entomol. Zool. 35 487–94
- [28] Khaheshi A and Rajabi H 2022 Mechanical intelligence (MI): a bioinspired concept for transforming engineering design Adv. Sci. 9 2203783
- [29] Jafarpour M, Aryayi M, Gorb S N and Rajabi H 2024 Double-spiral as a bio-inspired functional element in engineering design Sci. Rep. 14 29225
- [30] Zhang J, Yang H, Zhao Y, Yang J, Aydin Y O, Li S, Rajabi H, Peng H and Wu J 2024 Adaptive, rapid, and stable trident robotic gripper: a bistable tensegrity structure implementation *IEEE/ASME Trans. Mechatronics* (https://doi.org/10.1109/TMECH.2024.3516948)

- [31] Zhang J, Shi J, Huang J, Wu Q, Zhao Y, Yang J, Rajabi H, Wu Z, Peng H and Wu J 2023 *In situ* reconfigurable continuum robot with varying curvature enabled by programmable tensegrity building blocks *Adv. Intell. Syst.* 5 2300048
- [32] Zhang J, Li Y, Kan Z, Yuan Q, Rajabi H, Wu Z, Peng H and Wu J 2023 A preprogrammable continuum robot inspired by
- elephant trunk for dexterous manipulation *Soft Robot.* **10** 636–46
- [33] Manoonpong P, Rajabi H, Larsen J C, Raoufi S S, Asawalertsak N, Homchanthanakul J, Tramsen H T, Darvizeh A and Gorb S N 2022 Fin ray crossbeam angles for efficient foot design for energy-efficient robot locomotion Adv. Intell. Syst. 4 2100133